Journal of Hazardous Materials 184 (2010) 561–566

Contents lists available at ScienceDirect

Journal of Hazardous Materials

journal homepage: www.elsevier.com/locate/jhazmat

Fabrication of FOX-7 quasi-three-dimensional grids of one-dimensional nanostructures via a spray freeze-drying technique and size-dependence of thermal properties

Bing Huang[a,b], Zhiqiang Qiao[c], Fude Nie[c], Minhua Cao[a,b,*], Jing Su[a,b], Hui Huang[c,**], Changwen Hu[a,b,*]

[a] Key Laboratory of Cluster Science, Ministry of Education of China, Department of Chemistry, Beijing Institute of Technology, Beijing 100081, PR China
[b] State Key Laboratory of Explosion Science and Technology, Beijing Institute of Technology, Beijing 100081, PR China
[c] Institute of Chemical Materials, China Academy of Engineering Physics, Mianyang 621900, PR China

ARTICLE INFO

Article history:
Received 6 June 2010
Received in revised form 18 August 2010
Accepted 18 August 2010
Available online 26 August 2010

Keywords:
FOX-7
Spray freeze-drying technique
Nanostructures
Size-dependence

ABSTRACT

1,1-Diamino-2,2-dinitroethylene ($C_2H_4N_4O_4$, FOX-7) quasi-three-dimensional (3D) grids, a promising high-energy-density material with superior sensitivity properties, were synthesized by a spray freeze-drying technique. The FOX-7 3D grids were constructed from one-dimensional nanostructures. The sizes and structures of the FOX-7 3D grids strongly depend on the concentration of the aqueous solution of FOX-7. A possible formation mechanism of this structure was proposed in detail. Thermal analysis reveals that decrease in average particle sizes of FOX-7 grids results in a lower decomposition temperature and a much higher decomposition rate, which is in agreement with those reported about inorganic nanomaterials.

1. Introduction

In recent years, 1,1-diamino-2,2-dinitroethylene ($C_2H_4N_4O_4$, FOX-7) has attracted considerable attention because of its excellent performance of high density and low sensitivity since it was reported in 1998 by the group from FOI [1]. Up to now, most of the researches have focused on the theoretical calculation, structural properties, improvement of synthesis routes, and study of thermolysis and sensitivity of FOX-7 microparticles [2–11], while few studies on FOX-7 nanostructures. However, similar to other inorganic nanostructures and organic nanostructures, energetic materials also exhibit some size-dependent properties, such as sensitivity, thermal stability, operational performance, and so on. For example, 1,3,5-trinitro-1,3,5-triazinane (RDX) nanopowders prepared by a sublimation/condensation process have a much higher burning rate than that of micro-sized ones [12]. Reticularly structured 1,3,5,7-tetranitro-1,3,5,7-tetrazocane (HMX) nanoparticles with a size of 50 nm have a lower impact sensitivity and lower temperature of the maximum energy release compared with conventional energetic materials [13]. 1,3,5-Triamino-2,4,6-trinitrobenzene (TATB) nanoparticles also have a lower temperature of the thermal decomposition and more weight loss, and short-pulse initiation threshold value of TATB nanoparticles-based explosives is evidently reduced [14]. Therefore, there is a need to develop a facile method for control of synthesis of FOX-7 nanostructures.

As well known, most of organic compounds feature van der Waals or other weak intermolecular interactions among molecules, which makes the synthesis of organic nanostructures more difficult than inorganic nanostructures with covalent bonds [15–17]. To date, there are only a few facile and simple approaches for the fabrication of micro/nanostructures of energetic and dangerous materials. Especially for FOX-7, to the best of our knowledge, the nano-sized structures of FOX-7 have not been reported yet. The reason is due in large part to its crystallographic structure. As shown in Fig. 1, similar to benzene in solid state, FOX-7 possesses a wavelike layered packing structure, and O and H atoms in the same layer are connected by hydrogen bonds. Thus it can be seen that the FOX-7 structure features the hydrogen-bond-aided π–π stacking, which may lead to the difficulty of the synthesis of FOX-7 nanostructures by conventional chemical methods.

Spray freeze-drying (SFD) technique has been successfully and widely used in the preparation of biological medicaments [18] and inorganic materials with high porosity [19], which is considered as one of the best ways for the fabrication of micro/nanoparticles as a physical method. The particles obtained by this method generally possess intriguing advantages such as molecular scale

* Corresponding authors. Tel.: +86 10 68912631; fax: +86 10 68912631.
** Corresponding author. Tel.: +86 816 2485301; fax: +86 816 2485301.
E-mail address: caomh@bit.edu.cn (M. Cao).

0304-3894/$ – see front matter © 2010 Elsevier B.V. All rights reserved.
doi:10.1016/j.jhazmat.2010.08.072

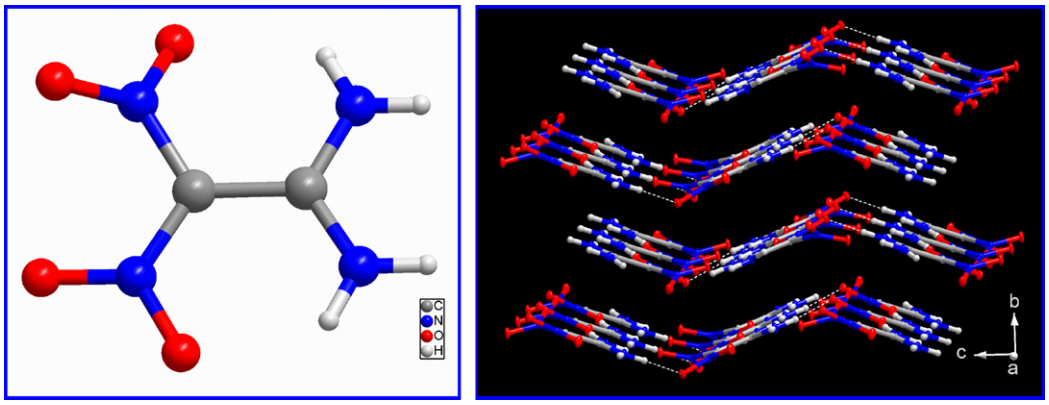

Fig. 1. (a) Planar structure and (b) layered structure of FOX-7. C, N, O, and H atoms are indicated in gray, blue, red, and white, respectively. (For interpretation of the references to colour in this figure legend, the reader is referred to the web version of the article.)

homogeneity because of flash freezing in the cryogen, and minimal agglomeration because of the sublimation of the water ice in the low-temperature vacuum drying process [20,21]. In this work, we first report the synthesis of FOX-7 three-dimensional (3D) grid nanostructures with different unit sizes by the freeze-drying technique mentioned above. The resulting FOX-7 3D structures are constructed from one-dimensional nanostructures. The size of the as-resulting nanostructures could be easily controlled by changing the concentration of raw material. A plausible formation mechanism of the FOX-7 grids is also proposed. In addition, studies on thermal properties of different-sized FOX-7 grids show that the decrease in average particle sizes results in a lower decomposing temperature and a much higher decomposition rate.

2. Experimental

2.1. Chemicals

Micro-sized FOX-7, which was synthesized by nitration of 4,6-dihydroxy-2-methylpyrimidine and subsequent hydrolysis of the resulting intermediate 2-dinitromethylene-5,5-dinitropyrimidine-4,6-dione [7], was recrystallized one time in 1-methyl-2-pyrrolidinone (NMP)/H_2O (70/30) and the purity was higher than 99.7%. Ultra-pure water (resistivity = 18.2 MΩ cm) was produced using a Milli-Q apparatus (Millipore) and filtered using an inorganic membrane with a pore size of 0.02 μm (Whatman International, Ltd.) just before use.

2.2. Preparation of FOX-7 quasi-three-dimensional grid nanostructures

The preparation process of FOX-7 3D grid nanostructures by the SFD technique is shown in Fig. 2. In a typical preparation, micro-sized FOX-7 as raw material was first added into 100 mL of ultra-pure water at 80 °C with constant stirring. After complete dissolution, the solution was quickly transferred into the spray chamber and sprayed with an air-atomization nozzle into the refrigerator containing liquid nitrogen to form droplets under stirring. Second, the droplets begin to freeze while passing through the cold vapor phase, and then completely froze after contacting with the liquid nitrogen. Finally, the dispersed frozen droplets were collected from the liquid nitrogen and transferred to the shelf of a pre-cooled Thermo Savant ModulyoD-230 (USA) freeze-dryer, and the water ice was sublimed from the frozen FOX-7 under a reduced pressure at −54 °C for 96 h. A green-yellow product was obtained. To elucidate the effect of the concentration of FOX-7 raw material on the size and morphology of final product, four different concentrations (C_{FOX-7} = 0.1, 0.2, 1, and 2 g/L, respectively), were used in our experiments and four samples were obtained and labeled as a–d.

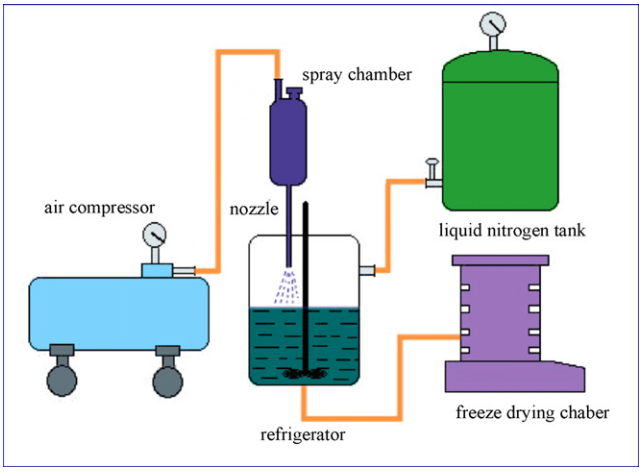

Fig. 2. Flow chart of the FOX-7 quasi-three-dimensional grids fabricated via SFD technique.

2.3. Characterization

The overall crystallinity and phase composition of as-prepared samples were characterized by X-ray diffraction (XRD) with Cu Kα radiation (λ = 1.5418 Å) on a D8 Advance X-ray diffractometer. The morphology and size distribution of the products were analyzed by field emission scanning electron microscopy (FE-SEM) on a Nova 600i field emission microscope operated at an acceleration voltage of 15 kV. Thermal gravimetric and differential scanning calorimetric analyses (TG-DSC) were carried out on a Simultaneous DSC-TG (SDT) Q600 unit in the N_2 atmosphere with a heating rate of 10 K/min.

3. Results and discussion

3.1. Composition of the samples

X-ray powder diffraction (XRD) pattern shows that the micro-FOX-7 raw material as-used exhibits a high crystallinity (Fig. 3A(e)). The samples obtained by the SFD technique with different concentrations of micro-FOX-7 exhibit almost same XRD patterns (Fig. 3A(a–d)), and are in good agreement with the raw material. It indicates high stability of FOX-7 under the SFD process and no detectable impurities from decomposition of FOX-7 were

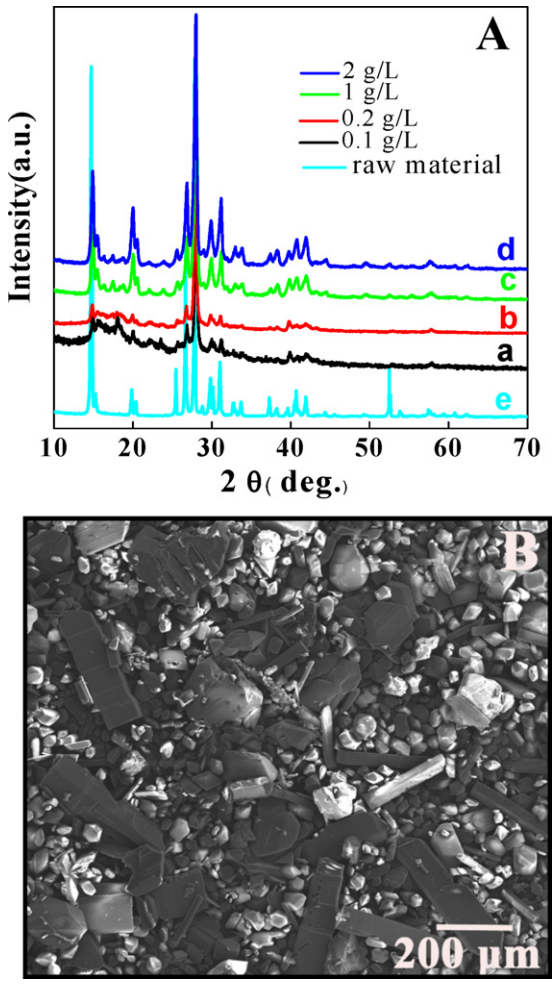

Fig. 3. (A) XRD pattern and (B) SEM image of micro-FOX-7 raw material.

produced. Furthermore, the diffraction peaks gradually sharpen with the increase of the concentration of FOX-7 raw material, demonstrating that higher concentration of raw material favors the formation of highly crystalline product.

In our experiment, the used micro-FOX-7 raw material is first characterized by X-ray powder diffraction (XRD) and field emission scanning electron microscopy (FE-SEM) to determine its crystallinity, size, and morphology, as shown in Fig. 3. It has been seen from Fig. 3A(e) and B that the used raw material exhibits a high crystallinity and a non-uniform particle size distribution, ranging from 50 to 200 μm. The overall crystallinity and composition of the samples prepared by the SFD technique were also examined by XRD measurements. As shown in Fig. 3A(a–d), the samples obtained with different concentrations of micro-FOX-7 exhibit almost same XRD patterns, in good agreement with that of the raw material. So it can be concluded that no detectable impurities were produced by this SFD technique. Furthermore, it can be clearly seen that with the increase of the concentration of FOX-7 raw material, the diffraction peaks gradually sharpen, indicating that higher concentration of raw material favors the formation of highly crystallized product.

3.2. Morphologies of the typical nanostructures

Field emission scanning electron microscopy (FE-SEM) image reveals non-uniform particle size distribution of the raw material ranging from 50 to 200 μm (Fig. 3B). The size and morphology of the as-prepared samples were characterized by FE-SEM measurements. Fig. 4 shows FE-SEM images of the samples obtained with SFD technique with different concentrations of FOX-7 raw material. When $C_{FOX\text{-}7}$ = 0.1 g/L was used, it can be seen from the low magnification FE-SEM image (Fig. 4a) that the sample exhibits a clear 3D grid structure. Fig. 4b shows a higher magnification FE-SEM of the same sample, from which it can be found that the 3D grids are constructed via crossed one-dimensional nanowires with ~100 nm in diameter. In addition, nanoparticles attaching on the grids are occasionally observed. When $C_{FOX\text{-}7}$ was increased to 0.2 g/L, the 3D grids almost cannot be observed, as shown in Fig. 4c. From the higher magnification FE-SEM image (Fig. 4d), many irregular particles with ~160 nm in diameter instead of three-dimensional grids were formed and 3D grids could be seen only in small region. With further increase of $C_{FOX\text{-}7}$ to 1.0 and 2.0 g/L, 3D grids completely disappear and relatively regular particles are formed with a size of 300 nm for $C_{FOX\text{-}7}$ = 1.0 g/L (Fig. 5a and b) and irregular particles with a size range of 200–800 nm for $C_{FOX\text{-}7}$ = 2.0 g/L (Fig. 5c and d), respectively. As a result, it can be seen that lower concentration of FOX-7 raw material favors the formation of quasi-three-dimensional grids of one-dimensional nanostructures, while higher concentration easily leads to the formation of larger nanoparticles. The possible mechanism will be discussed below.

3.3. Formation mechanism of the FOX-7 quasi-three-dimensional grids

Based on above SEM observation, a possible formation mechanism of FOX-7 quasi-three-dimensional grids was proposed, and a scheme was summarized in Fig. 6. When lower concentration of FOX-7 aqueous solution is sprayed into liquid nitrogen, a high degree of super-cooling leads to a high nucleation rate and small particles and ice were rapidly formed due to the rapid heat transfer between the aqueous solution and the cryogen. Thus the formed ice limited the aggregation of small particles. After sublimation of the ice, small particles with a relatively high energy started to aggregate by self-assembly, leading to the formation of quasi-three-dimensional grid structures, as shown in Fig. 6 (upper route). For concentrated solution, larger particles were obtained in the same volume compared with the dilution solution after the aqueous solution was injected into liquid nitrogen. Contrary to the case for the dilution solution, the self-assembly process did not happen after sublimation of the ice due to the high stability of the larger particles and thus the grid network structures did not form, but leading to the formation of irregular particles as shown in Fig. 6 (lower route).

3.4. Thermal analysis study of FOX-7 nanostructures

The thermal properties of the as-prepared FOX-7 nanostructures were investigated using thermogravimetry (TGA) and differential scanning calorimetry (DSC) measurements. As shown in Fig. 7A, the DSC patterns of both the as-prepared FOX-7 nanostructures and raw material all show two exothermal peaks with the maximum in the range of 240–256 °C and 280–298 °C, respectively. The first one can be elucidated by the fact that the emergence of nitro-to-nitrite rearrangement in this molecule leads to the destruction of conjugated system and hydrogen bonds and thus the fracture of nitro– leads to the formation of nitrogen monoxide (NO) [22]. Furthermore, it can be clearly seen that this exothermal peak shifts toward higher temperature with the decrease of FOX-7 particle sizes. This phenomenon can be explained by the theory of topochemical reactions [23]. It is well known that there are many lattice defects on the surfaces of the bigger crystals and these lattice defects could act as the active centers, on which condensed-phase products are formed. The existence of the condensed-phase prod-

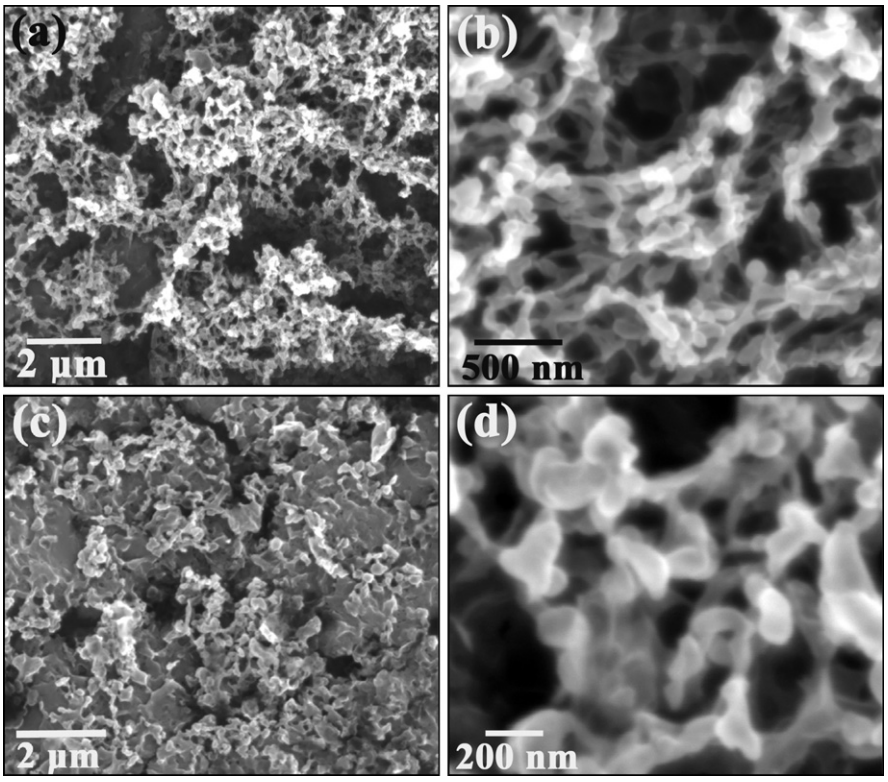

Fig. 4. (a) Low magnification; (b) high magnification of FE-SEM images of FOX-7 nanostructures prepared with $C_{FOX\text{-}7}$ = 0.1 g/L; (c) low magnification; (d) high magnification of FE-SEM images of FOX-7 nanostructures prepared with $C_{FOX\text{-}7}$ = 0.2 g/L.

ucts on the crystal surfaces results in an additional internal stress and as a consequence the crystals break into pieces. The repeating occurrence of this process makes FOX-7 bigger crystals partly decompose, leading to the formation of small crystals. In contrast, the small sized FOX-7 particle generally requires a higher decomposition temperature because of its less lattice defects and smaller internal stress. In addition, it is interesting to note that the first exothermal peak of the smallest sized particles (Fig. 7A(a)) is hardly

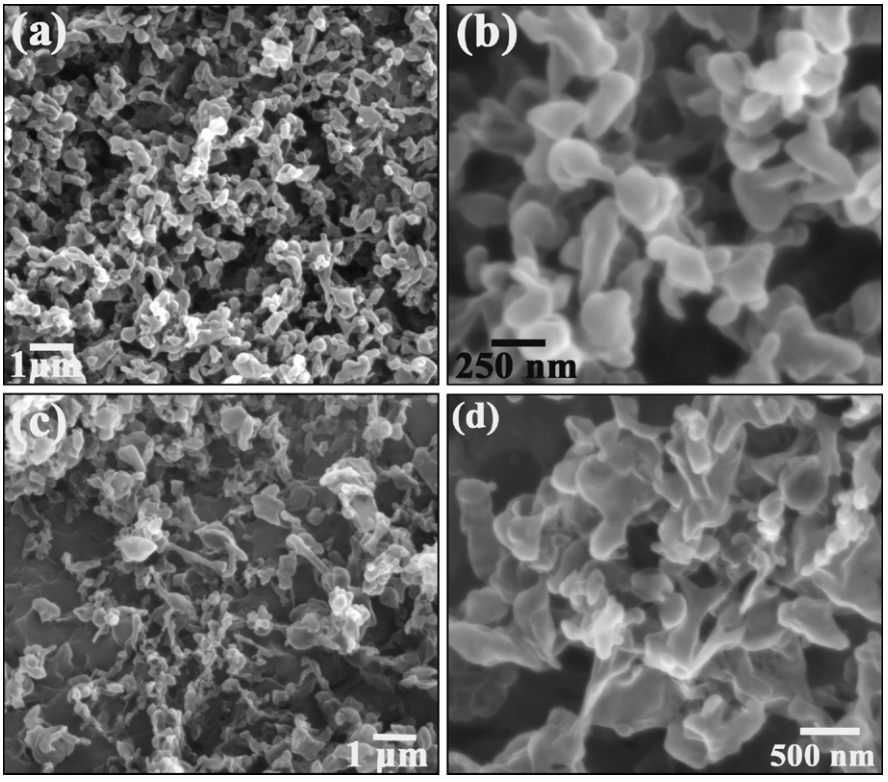

Fig. 5. (a) Low magnification; (b) high magnification of FE-SEM images of FOX-7 nanostructures prepared with $C_{FOX\text{-}7}$ = 1 g/L; (c) low magnification; (d) high magnification of FE-SEM images of FOX-7 nanostructures prepared with $C_{FOX\text{-}7}$ = 2 g/L.

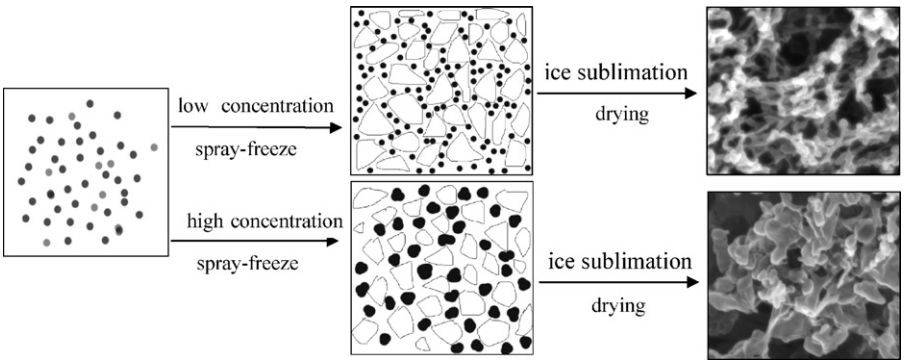

Fig. 6. A probable formation process of FOX-7 network structures under the same super-cooling rate.

observed. That may be due to the fact that accumulated heat effects can be dispersed effectively due to the higher surface area of the small sized FOX-7 nanostructures and thus the first decomposition cannot occur. For the second exothermal peak, it can be ascribed to the fracture of carbon skeleton in FOX-7 molecule, and this peak shifts toward lower temperature with the decrease of the particle size. There is a shift of approximate 13 °C toward lower temperature compared as-synthesized FOX-7 nanostructures with the smallest size with mirco-FOX-7. This result reveals that the decrease in average particle sizes leads to a lower decomposing temperature. This is probably due to that decrease of the size of FOX-7 particles to nanometer range increases the ratio of surface atoms to interior atoms significantly. The small sized particles possess thus a higher surface energy, which may result in the decrease of decomposition temperature. Fig. 7B shows the TG curves of as-prepared FOX-7 nanostructures and raw material, all of which exhibit a distinct weight loss. When the particle size reduces to nanoscale, no evident inflexion is observed. It suggests that compared with micro-sized raw material, nano-sized FOX-7 has a much higher decomposition rate, which is in accordance with the results of DSC. Moreover, study on the electrostatic spark sensitivity of nano-FOX-7 obtained with the concentration of 2.0 g/L indicates that its 50% critical ignition voltage (V_{50}) and 50% critical ignition energy (E_{50}) are 13.19 kV and 2.65 J, respectively, which are lower than those of FOX-7 raw material, 16.42 kV and 4.11 J. The decrease may be explained by the possibility that the FOX-7 nanoparticles with a higher surface energy are easy to be stimulated.

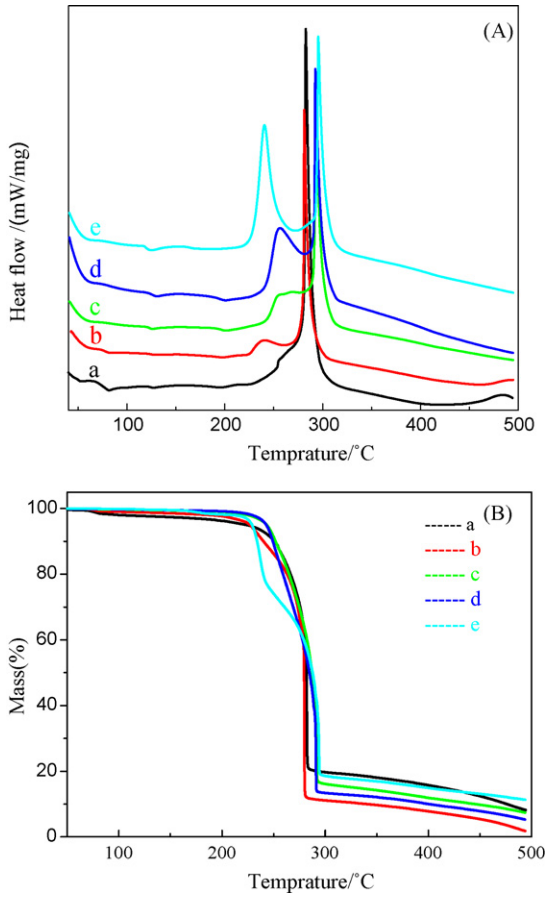

Fig. 7. DSC (A) and TGA (B) curves of FOX-7 nanostructures (a–d) and FOX-7 raw material (e) between 40 °C and 500 °C at a heating rate of 10 °C/min.

4. Conclusion

FOX-7 3D grid nanostructures with different unit sizes were first synthesized by a freeze-drying technique. The size of FOX-7 nanostructures was tunable by controlling the aqueous solution concentration of micro-FOX-7. The as-synthesized nanostructures exhibit size-dependence of thermal properties. This simple synthesis strategy may represent a general approach for the preparation of nanostructures of other water-solubility organic molecules.

Acknowledgements

This work was supported by the Natural Science Foundation of China (NSFC, Nos. 20731002, 10876002, 20771022, 20973023 and 91022006), the 111 Project (B07012), Program for New Century Excellent Talents in University, Open Fund of State Key Laboratory of Explosion Science and Technology and Beijing Institute of Technology (Nos. ZDKT08-01 and YBKT09-13), Specialized Research Fund for the Doctoral Program of Higher Education (SRFDP, No. 200800070015), Funding Project for Science and Technology Program of Beijing Municipal Commission (No. Z09010300820902), and the Key Foundation of China Academy of Engineering Physics (No. 2009A0302017).

References

[1] N.V. Latypov, J. Bergman, A. Langlet, U. Wellmar, U. Bemm, Synthesis and reactions of 1,1-diamino-2,2-dinitroethylene, Tetrahedron 54 (1998) 11525–11536.
[2] B. Janzon, H. Bergman, C. Eldsäer, C. Lamnevik, H. Ötmark, FOX-7—a novel, high performance, low vulnerability high explosive for warhead applications, in: Proceedings of the 20th International Symposium on Ballistics, Orlando, FL, USA, September 23–27, 2002, pp. 686–693.
[3] D.C. Sorescu, J.A. Boatz, D.L. Thompson, Classical and quantum-mechanical studies of crystalline FOX-7 (1,1-diamino-2,2-dinitroethylene), J. Phys. Chem. A 105 (2001) 5010–5021.
[4] J. Evers, T.M. Klapötke, P. Mayer, G. Oehlinger, J. Welch, α- and β-FOX-7, polymorphs of a high energy density material, studied by X-ray single crystal and

powder investigations in the temperature range from 200 to 423 K, Inorg. Chem. 45 (2006) 4996–5007.
[5] A.J. Bellamy, FOX-7 (1,1-diamino-2,2-dinitroethene), Struct. Bond. 125 (2007) 1–33.
[6] Z. Chyłek, S. Cudziło, J. Błądek, S. Pietrzyk, Optimization of 1,1-diamino-2,2-dinitroethene synthesis, Biul. WAT 53 (2005) 633 (in Polish).
[7] N.V. Latypov, M. Johansson, E. Holmgren, E.V. Sizova, V.V. Sizov, A.J. Bellamy, On the synthesis of 1,1-diamino-2,2-dinitroethene (FOX-7) by nitration of 4,6-dihydroxy-2-methylpyrimidine, Org. Process Res. Dev. 11 (2007) 56–59.
[8] M. Anniyappan, M.B. Talawar, G.M. Gore, S. Venugopalan, B.R. Gandhe, Synthesis, characterization and thermolysis of 1,1-diamino-2,2-dinitroethylene (FOX-7) and its salts, J. Hazard. Mater. B 137 (2006) 812–819.
[9] S. Karlsson, H. Ostmark, C. Eldsater, T. Carlsson, H. Bergman, S. Wallin, A. Pettersson, Detonation and sensitivity properties of FOX-7 and formulations containing FOX-7, in: Proceedings of 12th Symposium (International) on Detonation, San Diego, CA, USA, August 11–16, 2002, p. 5.
[10] H. Bergman, K. Ostmark, A. Pettersson, M.L. Pettersoon, U. Bemm, M. Hihkio, Some initial properties and thermal stability of FOX-7, in: Proceedings of the Symposium on Insensitive Mun. Energy Materials Technology, Tampa, USA, 1999, pp. 346–351.
[11] H. Östmark, H. Bergman, U. Bemm, P. Goede, E. Holmgren, M. Johansson, Langlet, N.V. Latypov, A. Pettersson, M.L. Petterson, N. Wingborg, C. Vörde, H. Stenmark, L. Karlsson, M. Hohkiö, 2,2-Dinitro-ethene-1,1-diamine (FOX-7)—properties, analysis, and scale-up, in: Proceedings of the 32nd International Annual Conference of ICT, Karlsruhe, Germany, 2001.
[12] Y. Frolov, A. Pivkina, P. Ulyanova, S. Zavyalov, Nanomaterials and nanostructures as components for high-energy condensed systems, in: Proceedings of 28th Int. Pyrotech. Semin., 2001, pp. 311–314.
[13] Y.X. Zhang, D.B. Liu, C.X. Lv, Preparation and characterization of reticular nano-HMX, Prop. Explos. Pyrotech. 30 (2005) 438–441.
[14] G.C. Yang, F.D. Nie, H. Huang, L. Zhao, W.T. Pang, Preparation and characterization of nano-TATB explosive, Prop. Explos. Pyrotech. 31 (2006) 390–394.
[15] X.J. Zhang, X.H. Zhang, W.S. Shi, X.M. Meng, C.S. Lee, S.T. Lee, Single-crystal organic microtubes with a rectangular cross section, Angew. Chem. Int. Ed. 46 (2007) 1525–1528.
[16] R.O. Al-Kaysi, C.J. Bardeen, General method for the synthesis of crystalline organic nanorods using porous alumina templates, Chem. Commun. (2006) 1224–1226.
[17] H.B. Liu, Y.L. Li, S.Q. Xiao, H.Y. Gan, T.G. Jiu, H.M. Li, L. Jiang, D.B. Zhu, D.P. Yu, B. Xiang, Y.F. Chen, Synthesis of organic one-dimensional nanomaterials by solid-phase reaction, J. Am. Chem. Soc. 125 (2003) 10794–10795.
[18] Y.F. Maa, P.A. Nguyen, T. Sweeney, S.J. Shire, C.C. Hsu, Protein inhalation powders: spray drying vs spray freeze drying, Pharm. Res. 16 (1999) 249–254.
[19] S. Kaluza, M. Muhler, On the precipitation mechanism and the role of the post-precipitation steps during the synthesis of binary $ZnO–Al_2O_3$ composites with high specific surface area, J. Mater. Chem. 19 (2009) 3914–3922.
[20] M.D. Rigterink, Advances in technology of the cryochemical process, Am. Ceram. Soc. Bull. 51 (1972) 158–161.
[21] P.J. McGrath, R.M. Laine, Theoretical process development for freeze-drying spray-frozen aerosols, J. Am. Ceram. Soc. 75 (1992) 1223–1228.
[22] A. Gindulyte, L. Massa, Proposed mechanism of 1,1-diamino-dinitroethylene decomposition: a density functional theory study, J. Phys. Chem. A 103 (1999) 11045–11051.
[23] E.A. Prodan, Localization phenomena of topochemical reactions, J. Therm. Anal. 29 (1984) 941–948.